
ZERO-SHOT SELF-CONSISTENCY LEARNING FOR SEISMIC IRREGULAR SPATIAL SAMPLING RECONSTRUCTION

A PREPRINT

Junheng Peng

The Key Laboratory of Earth Exploration
& Information Techniques of Ministry Education,
Chengdu, China
pengjunheng@stu.cdut.edu.cn

Yingtian Liu

School of Geophysics,
Chengdu University of Technology,
Chengdu, China
yingtianliu06@outlook.com

Mingwei Wang

School of Geophysics,
Chengdu University of Technology,
Chengdu, China
WangMingwei023478@outlook.com

Yong Li*

School of Geophysics,
Chengdu University of Technology,
Chengdu, China
liyong07@cdut.edu.cn

Huating Li

School of Geophysics,
Chengdu University of Technology,
Chengdu, China
lihuating@stu.cdut.edu.cn

November 5, 2024

ABSTRACT

Seismic exploration is currently the most important method for understanding subsurface structures. However, due to surface conditions, seismic receivers may not be uniformly distributed along the measurement line, making the entire exploration work difficult to carry out. Previous deep learning methods for reconstructing seismic data often relied on additional datasets for training. While some existing methods do not require extra data, they lack constraints on the reconstruction data, leading to unstable reconstruction performance. In this paper, we proposed a zero-shot self-consistency learning strategy and employed an extremely lightweight network for seismic data reconstruction. Our method does not require additional datasets and utilizes the correlations among different parts of the data to design a self-consistency learning loss function, driving a network with only 90,609 learnable parameters. We applied this method to experiments on the USGS National Petroleum Reserve–Alaska public dataset and the results indicate that our proposed approach achieved good reconstruction results. Additionally, our method also demonstrates a certain degree of noise suppression, which is highly beneficial for large and complex seismic exploration tasks.

Keywords Zero-shot Learning · Self-consistency · Seismic Data Reconstruction

1 Introduction

Over the past few decades, seismic exploration has been one of the most effective means of understanding subsurface structures, achieving significant success in fields such as oil and gas development Malehmir et al. [2012], regional geological studies Shen et al. [2024], and crustal research Tuve et al. [1954]. Seismic exploration mainly analyzes the

*Corresponding Author

reflected or refracted waves from underground, and their reception requires the arrangement of receivers along the survey line on the surface. However, the conditions on the surface are always very complex, and the undulations of the terrain and the distribution of surface objects can pose significant challenges to the layout of the entire observation system. By using some proposed methods, we can eliminate the impact of terrain variations on observation data; these methods are typically referred to as static correction Cox [1999]. Besides, there is usually another situation: due to various surface conditions, such as obstacles or areas with restricted access, some area in the exploration region may not be able to accommodate the deployment of receivers, resulting in an irregular spatial arrangement of the observation system Chen et al. [2019]. The seismic data observed by receivers with irregular spatial distribution is incomplete, which can severely hinder subsequent data processing and even the entire seismic exploration work.

To address this issue of reconstructing seismic data from irregular spatial sampling, many researchers have proposed a variety of methods. Various methods based on sparse transformations are the most widely used approaches Candès et al. [2006]. The assumption is that complete regular sampling of seismic data can be sparsely represented, while irregular spatial sampling affects this sparsity, resulting in many small amplitude coefficients in the sparse domain. By filtering out the small amplitude coefficients, reconstruction of the seismic data can be achieved. Typically, to achieve satisfactory results, the above steps need to be repeated multiple times. For such methods, they can be classified based on the type of sparse transformation basis functions, including Fourier transform Sacchi et al. [1998], curvelet transform Candès et al. [2006], wavelet transform Antonini et al. [1992], etc, and different choices exhibit varying sparse representation performance. In addition to using fixed basis functions, many researchers have proposed using learnable basis functions as an alternative, those methods commonly referred to as dictionary learning Kreutz-Delgado et al. [2003] Tošić and Frossard [2011]. However, the greatest challenge of methods based on sparse transformations lies in the filtering of small amplitude coefficients, which typically relies on manually set parameters. Achieving satisfactory results often requires multiple iterations to determine the relevant parameters. Besides the aforementioned methods, methods based on rank-reduction have also received significant attention from researchers Trickett et al. [2010] Abbad et al. [2011] Huang et al. [2016]. These methods assume that seismic data possesses a low-rank structure, and irregular spatial sampling disrupts this low-rank structure, leading to an increase in the rank of the data. Singular value decomposition (SVD) is the most commonly used rank-reduction operator for extracting the singular matrix of seismic data, followed by imposing constraints on the singular values. These methods also face challenges related to parameter selection.

In recent years, deep learning LeCun et al. [2015] has been widely applied in various fields and such applications include image processing Tian et al. [2020], speech processing Wang and Chen [2018], and text translation, where deep learning has significantly improved performance and efficiency. Deep learning methods have also been widely applied in seismic data processing, including tasks such as noise attenuation Saad and Chen [2020] Chen and Sacchi [2015] Peng et al. [2024], fault identification Wu et al. [2019] Hu et al. [2020], and seismic reconstruction Ovcharenko and Hou [2020] Liu et al. [2022] Liu et al. [2021]. In a strict sense, most work using deep learning for seismic data reconstruction is not significantly different from seismic data noise processing. It treats the missing areas of data as targets for regression, effectively transforming the entire task into a regression problem. However, inspired by some works in the field of image generation Goodfellow et al. [2020] Ho et al. [2020], many researches have begun to introduce deep learning generative models into the seismic reconstruction domain Siahkoobi et al. [2018] Oliveira et al. [2018a] Deng et al. [2024]. Essentially, various traditional computational methods reconstruct seismic data by examining the internal relationships between observed data and the spatial relationships between observed and target data while the methods based on generative models treat the observed irregularly sampled data as constraints for generating seismic data in the missing areas Oliveira et al. [2018b] Chang et al. [2020]. One important reason for the success of deep learning is the use of additional datasets for training; the large training sets provide effective constraints for the model's parameters. However, due to the lack of interpretability, the blind use of additional data, even if it yields seemingly good results, makes it difficult to trust the outcomes. At the same time, the generalization and performance of various deep learning methods largely depend on the dataset, which greatly limits the application of deep learning approaches in the reconstruction of irregularly sampled seismic data.

Therefore, we believe that for the reconstruction of irregularly sampled seismic data, it is necessary to return to the intrinsic relationships within the data itself. To solve this, we proposed a new deep learning paradigm aimed at exploring these intrinsic relationships through simple deep learning model, called zero-shot self-consistency learning. The relationships within the data itself, which we refer to as self-consistency, are often difficult to measure directly. Besides, this self-consistency is independent of other data, so our proposed deep learning method does not require additional data for training, which is often referred to as zero-shot learning Pourpanah et al. [2022]. Zero-shot learning does not require a large amount of additional data to construct datasets, nor does it necessitate modeling numerous data features. As a result, the number of parameters can be significantly reduced compared to traditional deep learning methods Mansour and Heckel [2023]. We applied the proposed method to the USGS National Petroleum Reserve–Alaska Bird and Houseknecht [2002] Miller et al. [2000] seismic data to evaluate its performance. In the NPRA, we used seismic

data spanning approximately 2015 km, with a total recording time of about 91.6 hours. The results indicate that our proposed method can efficiently and effectively reconstruct complex and large seismic datasets, and we further observed its resistance to noise interference. This has very positive implications for large-scale seismic exploration projects, effectively addressing the data collection challenges posed by terrain limitations.

2 Results

2.1 Reconstruction performance

It is worth noting that prior to our proposed zero-shot self-consistency learning (ZS-SCL), many researchers had proposed various unsupervised methods to address the irregular spatial sampling issue of seismic data Hu et al. [2019] Saad et al. [2023] Kong et al. [2020]. Fundamentally, their objective functions can all be expressed as:

$$\theta = \arg \min_{\theta} \|N(d|\theta) * R - d\|_2^2 \quad (1)$$

where θ represents the parameters of the optimized deep learning model, d denotes the irregular spatially sampled seismic data, and R denotes the spatial sampling operator of the receivers. The mechanism of this learning strategy is not yet clear, and there are no constraints on the reconstructed data in its loss function, resulting in highly unstable performance. The ZS-SCL we proposed can significantly improve this issue, as shown in Fig 1. This is a field data, which has been used for theoretical testing in many noise processing Liao et al. [2023] Chen et al. [2016] and seismic data reconstruction Zhang et al. [2020] Jia and Ma [2017] tasks. We trained deep learning networks using ZS-SCL and traditional learning above, respectively, with a detailed description of the network architecture provided in the Methods section.

We randomly omitted 50% of the seismic traces to simulate the data with irregular spatial sampling, and as can be seen, the waveforms of the reflected waves from the subsurface in the irregularly sampled seismic data are highly discontinuous, making such data difficult to process and interpret further. As we had previously anticipated, traditional learning does not yield stable results, lacking horizontal continuity and containing numerous reconstruction errors. This instability can lead to errors in the later stages, resulting in incorrect assessments of subsurface structures and severely impacting the entire seismic exploration task. In contrast, the results obtained using the ZS-SCL strategy are closer to the ground truth, and the reconstruction of various subsurface structures is also more stable compared to traditional learning. As shown in the fourth column of Fig 1, a fault develops at a depth of about 1 km (with a seismic data time sampling interval of 4 ms). The reconstruction of this fault using traditional learning is much more chaotic, making accurate assessment impossible. In contrast, the results obtained with ZS-SCL clearly display the fault, closely matching the ground truth.

To further quantify this improvement, we used structural similarity (SSIM) for evaluation. On this dataset with 50% of the data randomly missing, the SSIM achieved by ZS-SCL is 0.7786, while traditional learning only reached a result of 0.7552. As encountered in many previous works, when there is excessive missing data in the seismic data, there is significant ambiguity, making it difficult to accurately reconstruct the seismic data. When the data is excessively missing and the structure is complex, it is challenging for ZS-SCL to achieve accurate results using the existing data. It is worth mentioning that in most scenarios of irregular spatial sampling, such as the three regions shown in Fig 1, ZS-SCL achieves better results than traditional learning. The SSIM values for ZS-SCL in the three regions are 0.8215, 0.7657, and 0.8427, while the corresponding results for traditional learning are 0.7813, 0.7254, and 0.7723, all significantly lower than those of ZS-SCL. Building on this, we expanded the evaluation of ZS-SCL, which will be presented in detail in the next section.

2.2 Application

To assess the application potential of ZS-SCL, we used seismic data from the National Petroleum Reserve–Alaska (NPRa) by the United States Geological Survey Miller et al. [2000]. We used the entire open dataset from NPRa to test the application potential of ZS-SCL, processing a total of 17 survey lines in the work area, with a combined length of approximately 2015km and a total seismic recording time of about 91.6 hours 2. The test results are shown in Table 1. We used three metrics to evaluate the effectiveness of seismic data reconstruction: 1. the commonly used SSIM metric; 2. the R^2 metric, which is frequently employed to assess regression models; 3. since field data inevitably contains some amount of random noise, we employed principal component analysis Chen et al. [2015] to estimate the standard deviation μ of the noise, which reflects its intensity.

We used an NVIDIA RTX 3060 to process the 17 survey lines and recorded the processing time; from an efficiency perspective, the lightweight network employed by ZS-SCL offers lower computational complexity. Notably, the original NPRa data contains strong random noise, which is an unavoidable issue in field seismic exploration work. In this

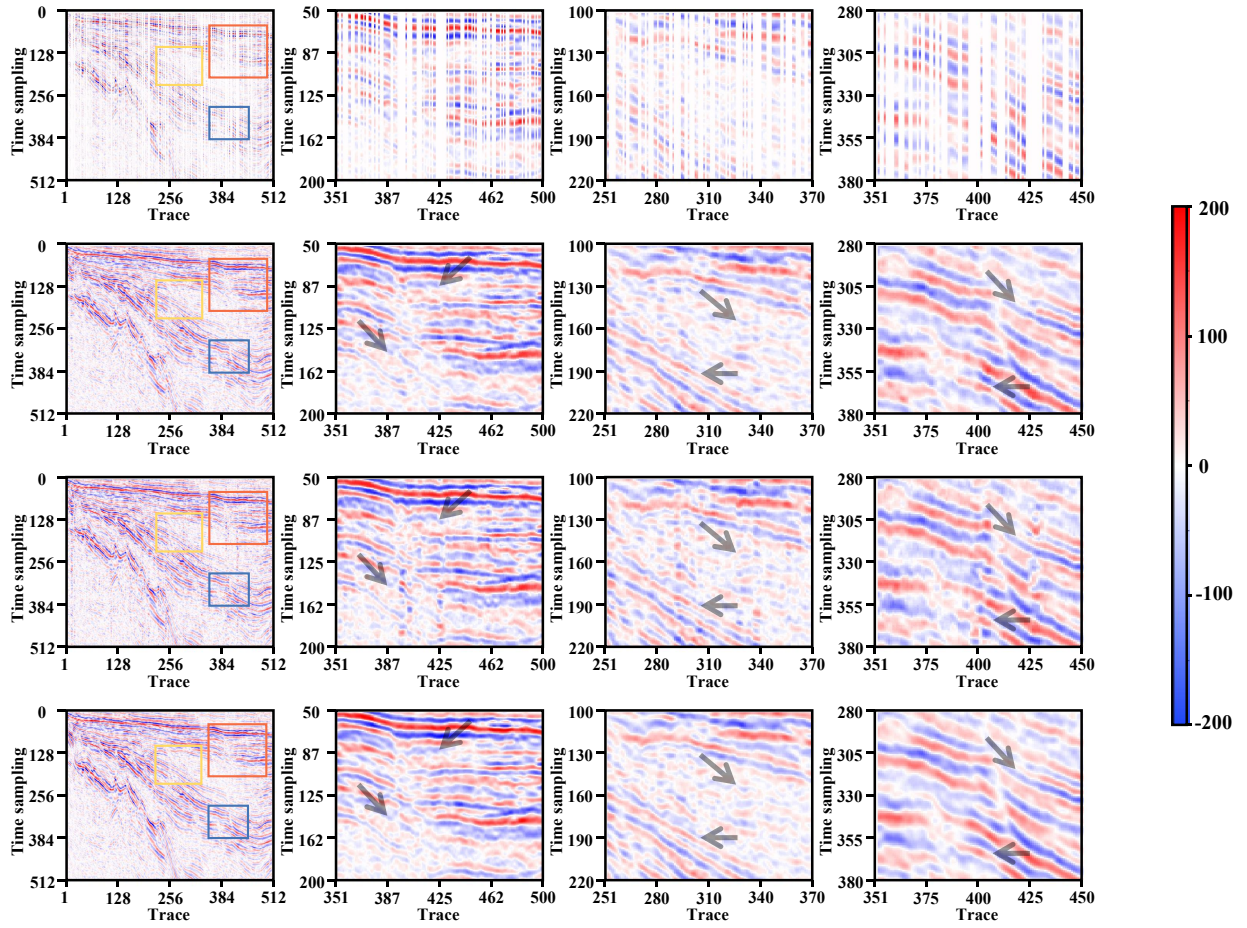


Figure 1: The first column, from top to bottom, represents the irregularly sampled seismic data with 50% randomly missing, the seismic data reconstructed using ZS-SCL, the seismic data reconstructed using traditional learning, and the fully sampled field data (ground truth). The second column shows an enlarged view of the red boxes in the first column, the third column shows an enlarged view of the yellow boxes in the first column, and the fourth column shows an enlarged view of the blue boxes in the first column.

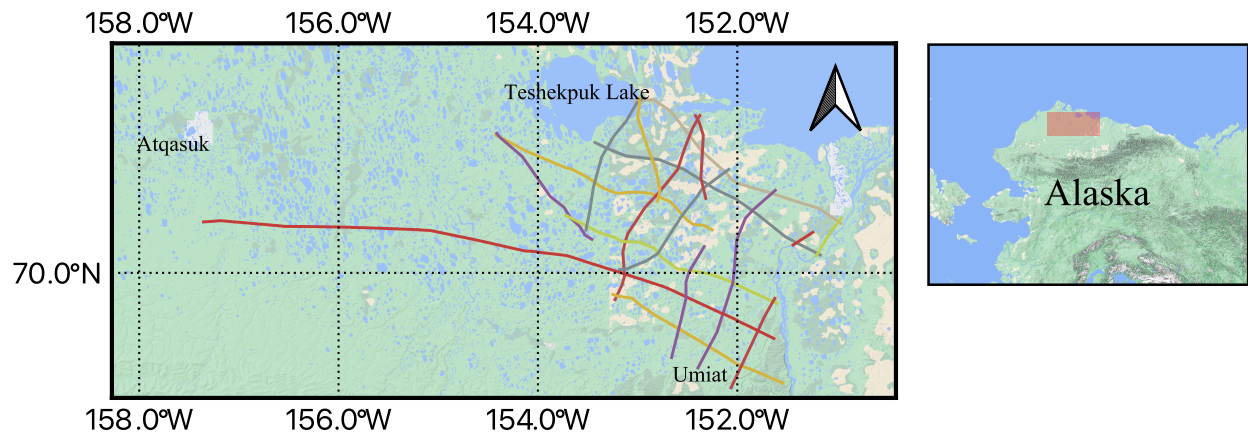


Figure 2: The location of our research area and lines.

| Survey Line | Original μ | 30% Missing | | | 50% Missing | | | Time Consumption |
|-------------|----------------|-------------|--------|--------|-------------|--------|--------|------------------|
| | | SSIM | R^2 | μ | SSIM | R^2 | μ | |
| Line 12 | 697.64 | 0.7488 | 0.9100 | 96.68 | 0.6763 | 0.8680 | 90.91 | 469s |
| Line 16 | 796.47 | 0.7619 | 0.9200 | 103.73 | 0.7085 | 0.8935 | 121.22 | 477s |
| Line 18 | 1668.54 | 0.7168 | 0.9024 | 83.56 | 0.6807 | 0.8748 | 100.90 | 463s |
| Line 22 | 638.34 | 0.7424 | 0.9169 | 75.17 | 0.6953 | 0.8871 | 55.72 | 274s |
| Line 27 | 1391.45 | 0.7638 | 0.9235 | 143.79 | 0.6984 | 0.8903 | 108.38 | 397s |
| Line 28 | 1535.42 | 0.7473 | 0.9224 | 78.40 | 0.6968 | 0.9006 | 71.50 | 445s |
| Line 31 | 894.85 | 0.7084 | 0.8997 | 132.57 | 0.6641 | 0.8845 | 173.63 | 53s |
| Line 33 | 272.84 | 0.7511 | 0.9190 | 143.63 | 0.6989 | 0.8894 | 98.92 | 274s |
| Line 34 | 1659.10 | 0.7289 | 0.9225 | 79.30 | 0.6959 | 0.9100 | 88.19 | 382s |
| Line 37 | 747.40 | 0.7616 | 0.9220 | 92.00 | 0.7135 | 0.8961 | 91.44 | 381s |
| Line 39 | 1511.08 | 0.7603 | 0.9317 | 88.74 | 0.7213 | 0.9097 | 96.94 | 189s |
| Line 41 | 2425.17 | 0.6046 | 0.8118 | 80.08 | 0.5578 | 0.7783 | 82.49 | 99s |
| Line 58 | 3182.10 | 0.3576 | 0.6085 | 483.66 | 0.3527 | 0.5894 | 387.68 | 147s |
| Line A | 1249.88 | 0.7871 | 0.9311 | 101.32 | 0.7296 | 0.8998 | 151.97 | 274s |
| Line B | 221.47 | 0.7607 | 0.9204 | 114.73 | 0.7120 | 0.8952 | 106.06 | 201s |
| Line C | 1540.40 | 0.7521 | 0.9280 | 106.79 | 0.7059 | 0.9068 | 78.47 | 234s |
| Line D | 1224.33 | 0.7779 | 0.9228 | 123.01 | 0.7229 | 0.8896 | 94.09 | 164s |

Table 1: The experimental results of 17 survey lines in NPRA. We randomly missed 30% and 50% of the data to construct irregular spatial sampling data and used SSIM, R^2 , and μ to evaluate the performance of ZS-SCL.

context, ZS-SCL still achieved very good results. In the reconstruction experiments with random missing data of 30% and 50%, both SSIM and R^2 remained at satisfactory levels. Additionally, thanks to the lightweight network we employed, ZS-SCL demonstrated satisfactory computational efficiency in processing the entire NPRA dataset, requiring only 1 hour and 22 minutes to handle data from 17 survey lines totaling 2015 km.

As examples, we presented data from survey lines 27 and 28, as shown in Fig 3, which contain a small amount of random noise. It can be observed that ZS-SCL achieved good results on both five data, successfully reconstructing nearly complete seismic data. However, a remaining issue with ZS-SCL is that when the missing data is too extensive, some horizontal discontinuities may still occur.

The reflected waves shown in the figure primarily originate from depths of 2 km to 5 km (with a time sampling interval of 4 ms). At this depth, the intensity of the deep reflections is weak, and the waveforms are complex. For these complex structures, ZS-SCL is able to achieve good reconstruction using only 50% of the seismic traces, which has very positive implications for the study of deep structures. On this basis, we extracted four seismic traces from each of the Line 27 and Line 28 for demonstration, as shown in Fig 4. The eight seismic lines we selected are distributed as evenly as possible in the spatial direction of the line. From the extracted seismic lines, it is clear that the reconstruction results of ZS-SCL are largely consistent with the ground truth, whether from strong reflections at shallow depths or weak reflections from deeper layers. It is important to note that NPRA’s data are limited by the collection environment and equipment, containing a certain amount of random noise, which is detrimental to subsequent data processing. Our proposed self-consistency learning assumes that different parts of the data can predict each other, allowing for overall modeling and reconstruction of the data. As is well known, random noise is unstructured and high-rank, making it difficult for deep learning networks like convolutional autoencoder, which perform data compression and reconstruction, to effectively reconstruct noise. Therefore, in the next section, we will discuss the application of ZS-SCL in the processing of noise in seismic data.

In summary, experiments on NPRA demonstrate the application potential of ZS-SCL. For many large work areas with complex surface conditions, it is not always feasible to deploy receivers for data collection, and a single side line can often produce a substantial amount of irregular spatial sampling data. Blindly using additional datasets in supervised deep learning methods can introduce external influences into the overall data reconstruction process, resulting in lower reliability of the reconstruction results. Moreover, the additional datasets directly affect the generalization capability of the deep learning network. Therefore, the selection of the training dataset significantly limits the application of supervised deep learning methods in field seismic exploration tasks. ZS-SCL employs a zero-shot learning strategy,

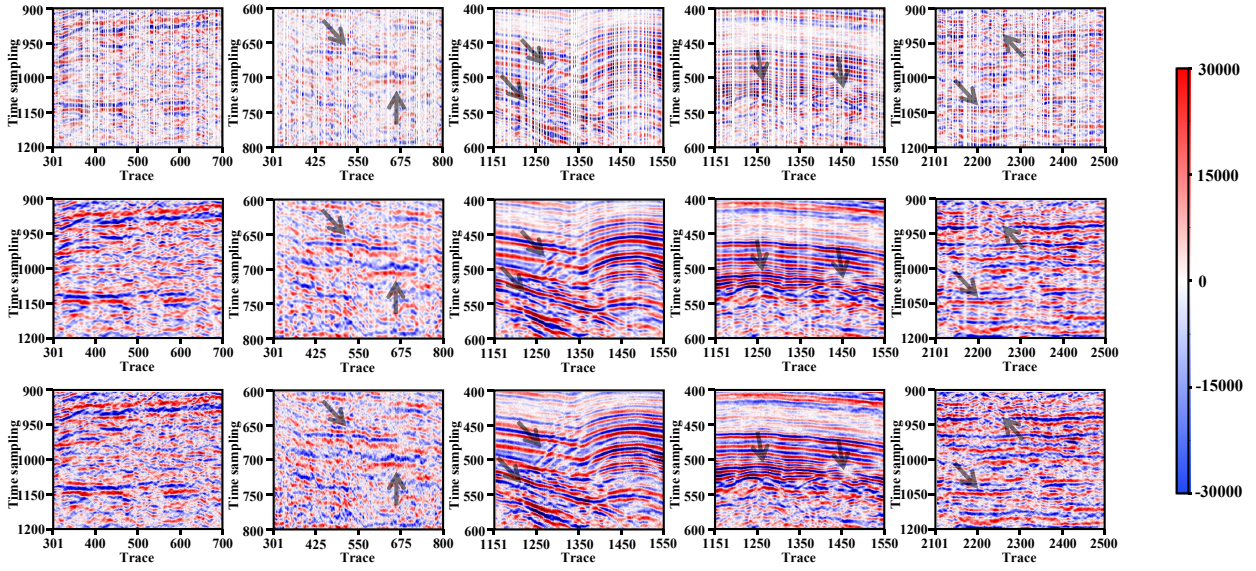


Figure 3: The first column represents the irregularly sampled data with 50% randomly missing, the second column shows the reconstructed data from ZS-SCL, and the third column displays the complete field data (ground truth).

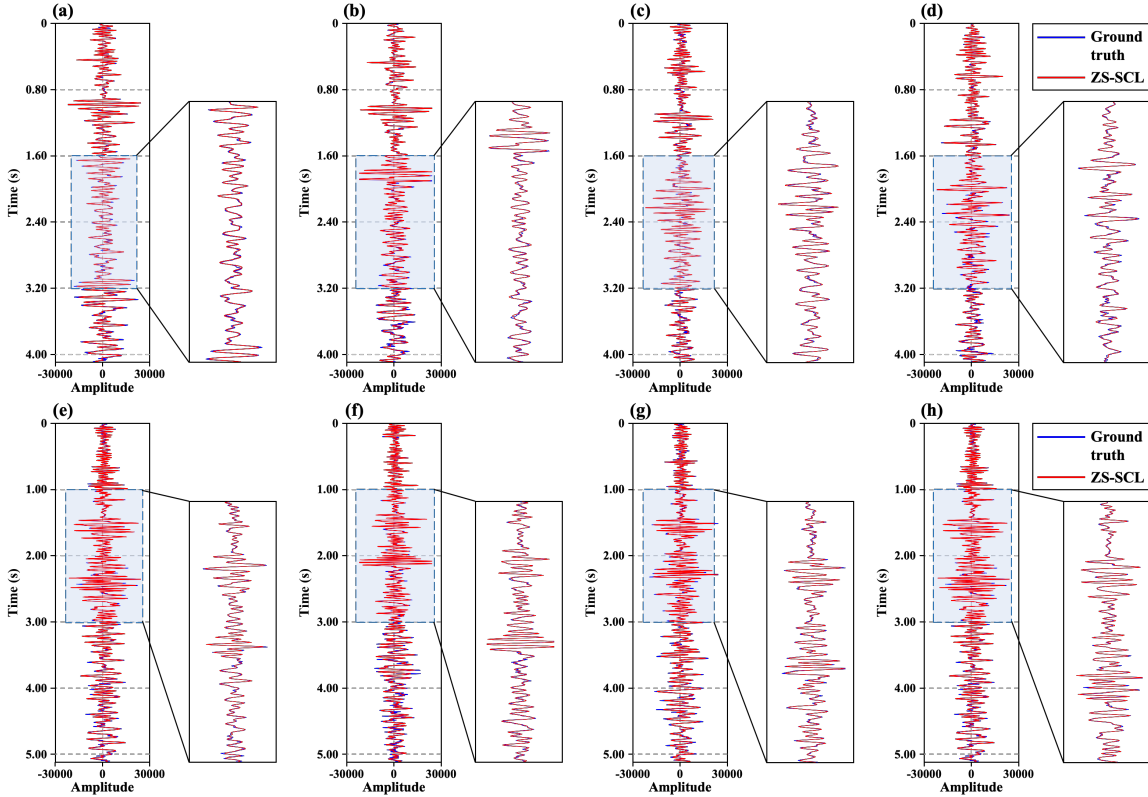


Figure 4: a), b), c) and d) represent the four seismic traces randomly extracted from Line 27; e), f), g) and h) represent the four seismic traces randomly extracted from Line 28.

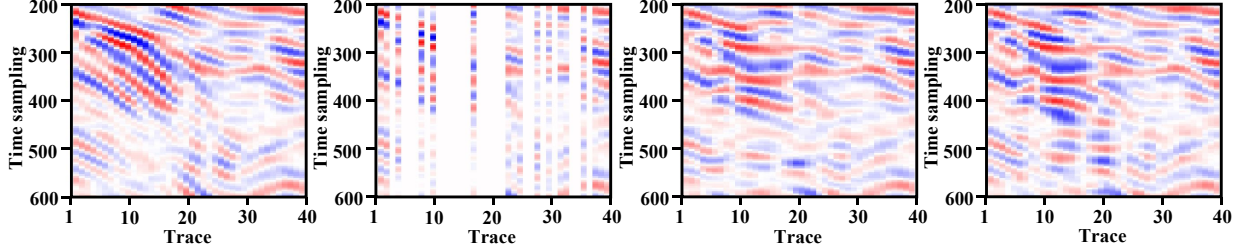


Figure 5: From left to right, they are: ground truth, irregularly sampled data, ZS-SCL processing results, and traditional learning processing results.

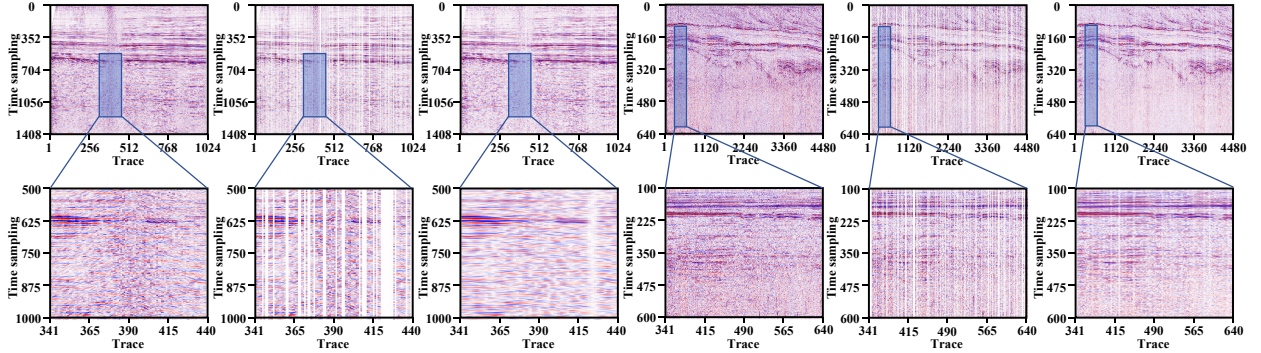


Figure 6: From left to right, the first to third columns represent the complete Line 41 data, the irregularly sampled Line 41 data with 30% randomly missing, and the data reconstructed by ZS-SCL, respectively; the fourth to sixth columns represent the complete Line 58 data, the irregularly sampled Line 58 data with 30% randomly missing, and the data reconstructed by ZS-SCL, respectively.

effectively avoiding the use of additional datasets, while the lightweight deep learning network used also maintains good processing efficiency, which has very positive implications for large-scale seismic exploration tasks. .

3 Discussion

Like many existing reconstruction methods, ZS-SCL also faces an almost intractable problem. Specifically, when certain subsurface features are completely missing, it is impossible to reconstruct them based solely on the available collected data. We selected a region from Fig 1 for demonstration, as shown in Fig 5. As can be seen, in this portion of the area, there is a significant amount of missing seismic traces, and the subsurface structure is very complex. In this case, even ZS-SCL struggles to perform accurate reconstruction, and similarly, traditional learning also fail to reconstruct it. This reconstruction bias has not been effectively addressed in existing research.

Furthermore, although ZS-SCL achieved good results in most of the NPRA measurement lines, the results in Line 41 and Line 58 were noticeably worse than in the other lines, as shown in Table 1. We conducted an in-depth investigation into the reasons for this performance decline. The reason for this phenomenon is that the signal-to-noise ratio of the NPRA data is not high, particularly evident in Line 41 and Line 58. As previously mentioned, ZS-SCL is unable to reconstruct unstructured random noise; therefore, the differences between the output results and the fully collected field data are mainly reflected in the noise. As shown in Fig 6, it can be observed that there is a significant amount of noise present in the original data for Line 41 and Line 58. It is evident that the fully collected data contains significant noise, which presents a major challenge for interpolation. However, when ZS-SCL processes the noisy irregularly sampled data, the level of noise in the reconstructed results decreases significantly. We believe that ZS-SCL's noise attenuation performance comes from two aspects. First, noise lacks structure, making it difficult to reconstruct random noise during the consistency learning. Second, the CAE deep learning architecture used exhibits some resistance to noise; it compresses the data before reconstruction, and since noise is high-frequency, the network struggles to reconstruct it effectively.

As the demand for understanding the earth’s deep structure increases, the need for large-scale seismic exploration tasks also rises. However, due to various limiting factors, the data obtained is often irregularly sampled in space and contains a certain amount of noise. ZS-SCL not only effectively reconstructs seismic data but also suppresses random noise in the data to some extent. Compared to traditional methods, ZS-SCL does not require parameter selection, does not rely on additional datasets for training, and its lightweight architecture effectively ensures processing efficiency. This offers new insights for seismic data reconstruction in large-scale exploration tasks.

4 Methods

According to the pioneering work on artificial intelligence, human intelligence is seen as a self-consistent system Lecky [1945], and this self-consistency aids in the structural modeling of external information. Therefore, based on this idea, we believe that self-consistency can be applied to the learning of deep learning networks, enhancing their learning efficiency and accuracy while enabling complete modeling of the data.

Our proposed method mainly consists of two parts: first, the zero-shot self-consistency learning, and second, the lightweight deep learning model that we employed. Typically, irregularly sampled seismic data can be represented as:

$$d = m * R \quad (2)$$

where d represents the observed seismic data, m is the complete seismic data need to be reconstructed, and R denotes the spatial sampling operator of the receivers. R is a matrix which contains only 0 and 1, and it is also a highly singular matrix. Therefore, the reconstruction of irregularly sampled seismic data cannot be solved directly by inverting the above equation.

4.1 Self-Consistency Learning

To address the aforementioned problem, we proposed the theory of self-consistency learning. We believe that there are varying degrees of correlation between the data received by different receivers. The reconstruction of seismic data is based on the relationship between the missing parts and the collected parts; if this relationship does not exist, the reconstruction task cannot be accomplished. Typically, due to the diversity of actual exploration scenarios, the relationships among different parts of the data are nonlinear and complex. Therefore, we proposed using deep learning method to learn these inherent latent relationships within the data.

We started from the classic objective function used in deep learning methods for seismic data reconstruction, which can be expressed as:

$$\theta = \arg \min_{\theta} \|N(d|\theta) * R - d\|_2^2 \quad (3)$$

where N represents a deep learning network and θ represents its learnable parameters. This objective function reconstructs seismic data by learning the compression and reconstruction of the collected data, and then utilizes the spatial relationship between the collected and missing data for the reconstruction. Clearly, it does not impose a direct constraint on the missing data, which is why instability in reconstruction results was observed in previous experiments. We believe that this issue can be addressed by imposing further constraints on N . Therefore, the aforementioned constraint can be further expressed as:

$$\theta = \arg \min_{\theta} (\|N(m * (1 - R)|\theta) * R - d\|_2^2 + \|N(d|\theta) * (1 - R) - m * (1 - R)\|_2^2) \quad (4)$$

This objective function consists of two parts. We aim to achieve bidirectional prediction of irregularly sampled seismic data through a deep learning network N , which means that the collected data can be used to reconstruct the missing data, while the missing data can also be utilized to reconstruct the collected data. However, m is the complete reconstructed seismic data we aim to obtain, so this objective function is self-contradictory.

To address this issue, our research approach is to approximate and substitute m . Assuming that the deep learning network N can effectively model the seismic data, it should satisfy the following:

$$m \approx N(d|\theta) \quad (5)$$

$$m \approx N(m * (1 - R)|\theta) \quad (6)$$

Integrating them, we can get:

$$N(d|\theta) \approx N(N(d|\theta) * (1 - R)|\theta) \quad (7)$$

which indicates that the reconstruction target for N is consistent and the learnable parameters θ of N should satisfy:

$$\theta = \arg \min_{\theta} \|N(d|\theta) - N(N(d|\theta) * (1 - R)|\theta)\|_2^2 \quad (8)$$

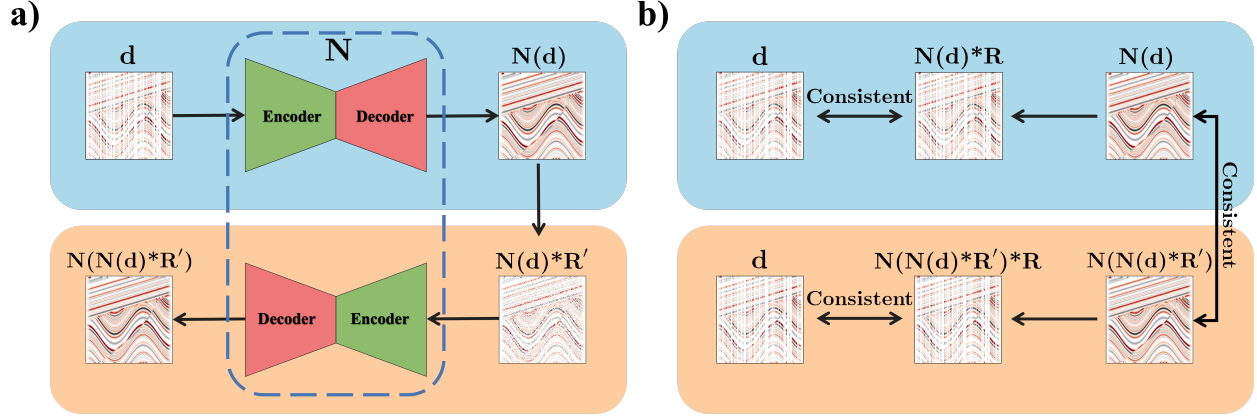


Figure 7: The overall process of zero-shot self-consistency learning. a) the deep learning network N is deployed twice during a single training process; b) the consistency among the input and outputs.

By substituting m into the improved constraint objective function 4 mentioned above, we can obtain:

$$\theta = \arg \min_{\theta} (\|d - N(d|\theta) * R\|_2^2 + \|d - N(N(d|\theta) * (1 - R))|\theta) * R\|_2^2 + \|N(d|\theta) - N(N(d|\theta) * (1 - R)|\theta)\|_2^2) \quad (9)$$

The above objective function is the self-consistency learning function we proposed, which effectively reflects the bidirectional relationship between the missing data and the collected data. To further enhance the deep learning network's overall modeling of the data, we randomly resampled a R' during each iteration of the learning process to replace $(1 - R)$ in the objective function. The purpose of using the aforementioned R' is that we hope N can establish not only the relationship between the missing seismic data and the collected seismic data, but also model the internal connections within the collected data and the missing seismic data respectively.

In summary, the self-consistency learning objective function proposed in this work can be expressed as:

$$\theta = \arg \min_{\theta} (\|d - N(d|\theta) * R\|_2^2 + \|d - N(N(d|\theta) * R')|\theta) * R\|_2^2 + \|N(d|\theta) - N(N(d|\theta) * R'|\theta)\|_2^2) \quad (10)$$

The aforementioned loss function can be achieved using a single field observation data without the need for an additional dataset, so it is also a form of zero-shot learning. The overall process is shown in Fig 7. As shown in the figure, our proposed zero-shot self-consistency learning strategy is driven solely by the internal correlations within the data itself, without the need for additional datasets. In the next section, we provided a detailed description of the lightweight deep learning network used in our work.

4.2 Deep Learning Network

In this work, we used a very simple deep learning model for validation. We adopted the structure of a convolutional autoencoder (CAE), as illustrated in Fig 8. The CAE has a very simple structure. First, encoder downsamples the input seismic data while continuously expanding its channels to encode the data. The encoded data is then decoded through a fully connected layer that operates along the channel dimension. During the decoding process, transposed convolution is used to compress the channels of the data, followed by continuous upsampling to reconstruct the data.

In zero-shot self-consistency learning, since it only requires fitting the consistency of a single irregularly sampled seismic dataset at a time, the number of parameters does not need to be very large. We conducted a large number of additional experiments, which showed that increasing the size of the network does not lead to performance improvements; instead, it significantly increases the complexity of training. In the CAE we used, the encoder consists of four convolutional layers, each with a kernel size of 4×4 . The decoder has a symmetrical structure to the encoder and uses four transposed convolutional layers for upsampling. The specific parameters of each structure in the CAE are shown in Table 2, and the total learnable parameters of the entire model are only 90,609, which is a decrease of several tens of times compared to some other traditional deep learning networks He et al. [2016] Ronneberger et al. [2015] Ulyanov et al. [2018].

With the development of deep learning, many backbone networks have been proposed by researchers, such as Transformer Vaswani [2017] and Kolmogorov-arnold networks Liu et al. [2024]. Future exploration can focus on pairing self-consistency learning with optimal deep learning networks.

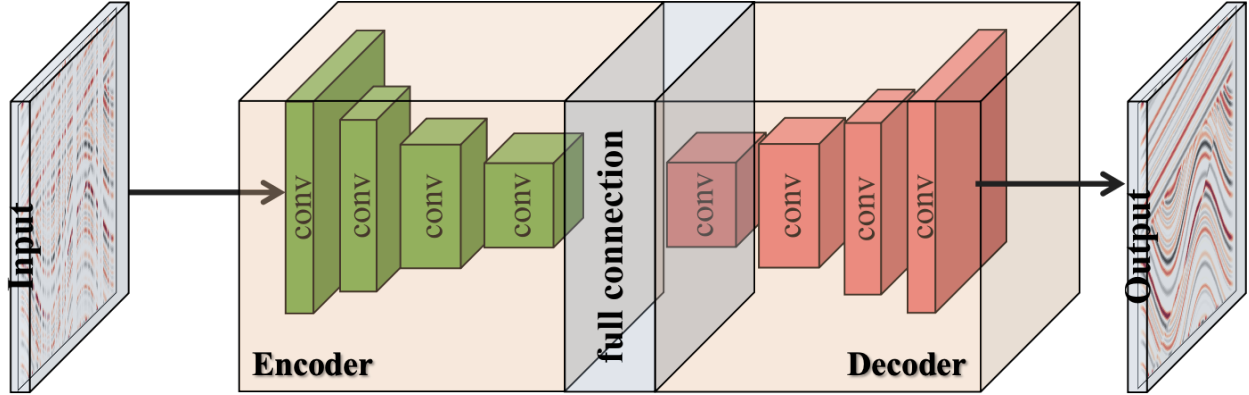


Figure 8: The deep learning network we used in this work has a autoencoder structure, which includes encoder, full connection layer and decoder.

| Hyper parameter | Setting |
|----------------------------|-----------------|
| Encoder Channels | [8, 16, 32, 64] |
| Full Connected Channels | 64 |
| Decoder Channels | [64, 32, 16, 8] |
| Total Learnable Parameters | 90609 |

Table 2: The parameters of CAE

Acknowledgements

We thank dGB Earth Sciences for making the data available as an OpendTect project via their TerraNubis portal terranubis.com.

Additional information

Data availability

The NPRA data we use can be found at: <https://terranubis.com/datainfo/USGS-Central-Alaska-2023>, which is a seismic exploration project led by USGS Bird and Houseknecht [2002] Miller et al. [2000].

Code availability

The code and data processing results in the article can be obtained by contacting the corresponding author.

References

- Alireza Malehmir, Raymond Durrheim, Gilles Bellefleur, Milovan Urosevic, Christopher Juhlin, Donald John White, Bernd Milkereit, and Geoff Campbell. Seismic methods in mineral exploration and mine planning: A general overview of past and present case histories and a look into the future. *Geophysics*, 77(5):WC173–WC190, 2012.
- Zhichao Shen, Yan Yang, Xiaojing Fu, Kyra H Adams, Ettore Biondi, and Zhongwen Zhan. Fiber-optic seismic sensing of vadose zone soil moisture dynamics. *Nature Communications*, 15(1):6432, 2024.
- Merle A Tuve, Howard E Tatel, and Pembroke J Hart. Crustal structure from seismic exploration. *Journal of Geophysical Research*, 59(3):415–422, 1954.
- Mike Cox. *Static corrections for seismic reflection surveys*. Society of Exploration Geophysicists, 1999.
- Yangkang Chen, Xiaohong Chen, Yufeng Wang, and Shaohuan Zu. The interpolation of sparse geophysical data. *Surveys in Geophysics*, 40:73–105, 2019.

- Emmanuel J Candès, Justin Romberg, and Terence Tao. Robust uncertainty principles: Exact signal reconstruction from highly incomplete frequency information. *IEEE Transactions on information theory*, 52(2):489–509, 2006.
- Mauricio D Sacchi, Tadeusz J Ulrych, and Colin J Walker. Interpolation and extrapolation using a high-resolution discrete fourier transform. *IEEE Transactions on Signal Processing*, 46(1):31–38, 1998.
- Emmanuel Candes, Laurent Demanet, David Donoho, and Lexing Ying. Fast discrete curvelet transforms. *multiscale modeling & simulation*, 5(3):861–899, 2006.
- Marc Antonini, Michel Barlaud, Pierre Mathieu, and Ingrid Daubechies. Image coding using wavelet transform. *IEEE Trans. Image Processing*, 1:20–5, 1992.
- Kenneth Kreutz-Delgado, Joseph F Murray, Bhaskar D Rao, Kjersti Engan, Te-Won Lee, and Terrence J Sejnowski. Dictionary learning algorithms for sparse representation. *Neural computation*, 15(2):349–396, 2003.
- Ivana Tošić and Pascal Frossard. Dictionary learning. *IEEE Signal Processing Magazine*, 28(2):27–38, 2011.
- Stewart Trickett, Lynn Burroughs, Andrew Milton, Larry Walton, and Rob Dack. Rank-reduction-based trace interpolation. In *SEG International Exposition and Annual Meeting*, pages SEG–2010. SEG, 2010.
- Brahim Abbad, Bjørn Ursin, and Milton J Porsani. A fast, modified parabolic radon transform. *Geophysics*, 76(1): V11–V24, 2011.
- Weilin Huang, Runqiu Wang, Yangkang Chen, Huijian Li, and Shuwei Gan. Damped multichannel singular spectrum analysis for 3d random noise attenuation. *Geophysics*, 81(4):V261–V270, 2016.
- Yann LeCun, Yoshua Bengio, and Geoffrey Hinton. Deep learning. *nature*, 521(7553):436–444, 2015.
- Chunwei Tian, Lunke Fei, Wenxian Zheng, Yong Xu, Wangmeng Zuo, and Chia-Wen Lin. Deep learning on image denoising: An overview. *Neural Networks*, 131:251–275, 2020.
- DeLiang Wang and Jitong Chen. Supervised speech separation based on deep learning: An overview. *IEEE/ACM transactions on audio, speech, and language processing*, 26(10):1702–1726, 2018.
- Omar M Saad and Yangkang Chen. Deep denoising autoencoder for seismic random noise attenuation. *Geophysics*, 85(4):V367–V376, 2020.
- Ke Chen and Mauricio D Sacchi. Robust reduced-rank filtering for erratic seismic noise attenuation. *Geophysics*, 80(1): V1–V11, 2015.
- Junheng Peng, Yong Li, Zhangquan Liao, Xuben Wang, and Xingyu Yang. Seismic data strong noise attenuation based on diffusion model and principal component analysis. *IEEE Transactions on Geoscience and Remote Sensing*, 2024.
- Xinming Wu, Luming Liang, Yunzhi Shi, and Sergey Fomel. Faultseg3d: Using synthetic data sets to train an end-to-end convolutional neural network for 3d seismic fault segmentation. *Geophysics*, 84(3):IM35–IM45, 2019.
- Guang Hu, Zhengwang Hu, Jiangping Liu, Fei Cheng, and Daicheng Peng. Seismic fault interpretation using deep learning-based semantic segmentation method. *IEEE Geoscience and Remote Sensing Letters*, 19:1–5, 2020.
- Oleg Ovcharenko and S Hou. Deep learning for seismic data reconstruction: opportunities and challenges. In *First EAGE digitalization conference and exhibition*, volume 2020, pages 1–5. European Association of Geoscientists & Engineers, 2020.
- Naihao Liu, Lukun Wu, Jiale Wang, Hao Wu, Jinghui Gao, and Dehua Wang. Seismic data reconstruction via wavelet-based residual deep learning. *IEEE Transactions on Geoscience and Remote Sensing*, 60:1–13, 2022.
- Qun Liu, Lihua Fu, and Meng Zhang. Deep-seismic-prior-based reconstruction of seismic data using convolutional neural networks. *Geophysics*, 86(2):V131–V142, 2021.
- Ian Goodfellow, Jean Pouget-Abadie, Mehdi Mirza, Bing Xu, David Warde-Farley, Sherjil Ozair, Aaron Courville, and Yoshua Bengio. Generative adversarial networks. *Communications of the ACM*, 63(11):139–144, 2020.
- Jonathan Ho, Ajay Jain, and Pieter Abbeel. Denoising diffusion probabilistic models. *Advances in neural information processing systems*, 33:6840–6851, 2020.
- Ali Siahkoobi, Rajiv Kumar, and F Herrmann. Seismic data reconstruction with generative adversarial networks. In *80th EAGE conference and exhibition 2018*, volume 2018, pages 1–5. European Association of Geoscientists & Engineers, 2018.
- Dario AB Oliveira, Rodrigo S Ferreira, Reinaldo Silva, and Emilio Vital Brazil. Interpolating seismic data with conditional generative adversarial networks. *IEEE Geoscience and Remote Sensing Letters*, 15(12):1952–1956, 2018a.
- Fei Deng, Shuang Wang, Xuben Wang, and Peng Fang. Seismic data reconstruction based on conditional constraint diffusion model. *IEEE Geoscience and Remote Sensing Letters*, 2024.

- Dario AB Oliveira, Rodrigo S Ferreira, Reinaldo Silva, and Emilio Vital Brazil. Interpolating seismic data with conditional generative adversarial networks. *IEEE Geoscience and Remote Sensing Letters*, 15(12):1952–1956, 2018b.
- Dekuan Chang, Wuyang Yang, Xueshan Yong, Guangzhi Zhang, Wenlong Wang, Haishan Li, and Yihui Wang. Seismic data interpolation using dual-domain conditional generative adversarial networks. *IEEE Geoscience and Remote Sensing Letters*, 18(10):1856–1860, 2020.
- Farhad Pourpanah, Moloud Abdar, Yuxuan Luo, Xinlei Zhou, Ran Wang, Chee Peng Lim, Xi-Zhao Wang, and QM Jonathan Wu. A review of generalized zero-shot learning methods. *IEEE transactions on pattern analysis and machine intelligence*, 45(4):4051–4070, 2022.
- Youssef Mansour and Reinhard Heckel. Zero-shot noise2noise: Efficient image denoising without any data. In *Proceedings of the IEEE/CVF Conference on Computer Vision and Pattern Recognition*, pages 14018–14027, 2023.
- Kenneth J Bird and David W Houseknecht. Us geological survey 2002 petroleum resource assessment of the national petroleum reserve in alaska (npra). Technical report, 2002.
- John J Miller, Warren F Agena, Myung W Lee, Frederick N Zihlman, John A Grow, David J Taylor, Michele Killgore, and Harold L Oliver. Regional seismic lines reprocessed using post-stack processing techniques: National petroleum reserve, alaska. Technical report, US Geological Survey,, 2000.
- L Hu, X Zheng, Y Duan, and X Yan. Unsupervised seismic data interpolation via deep convolutional autoencoder. In *81st EAGE Conference and Exhibition 2019*, volume 2019, pages 1–5. European Association of Geoscientists & Engineers, 2019.
- Omar M Saad, Sergey Fomel, Raymond Abma, and Yangkang Chen. Unsupervised deep learning for 3d interpolation of highly incomplete data. *Geophysics*, 88(1):WA189–WA200, 2023.
- Fantong Kong, Francesco Picetti, Vincenzo Lipari, Paolo Bestagini, Xiaoming Tang, and Stefano Tubaro. Deep prior-based unsupervised reconstruction of irregularly sampled seismic data. *IEEE Geoscience and Remote Sensing Letters*, 19:1–5, 2020.
- Zhangquan Liao, Yong Li, En Xia, Yingtian Liu, and Rui Hu. A twice denoising autoencoder framework for random seismic noise attenuation. *IEEE Transactions on Geoscience and Remote Sensing*, 61:1–15, 2023.
- Yangkang Chen, Jianwei Ma, and Sergey Fomel. Double-sparsity dictionary for seismic noise attenuation. *Geophysics*, 81(2):V103–V116, 2016.
- Hao Zhang, Xiuyan Yang, and Jianwei Ma. Can learning from natural image denoising be used for seismic data interpolation? *Geophysics*, 85(4):WA115–WA136, 2020.
- Yongna Jia and Jianwei Ma. What can machine learning do for seismic data processing? an interpolation application. *Geophysics*, 82(3):V163–V177, 2017.
- Guangyong Chen, Fengyuan Zhu, and Pheng Ann Heng. An efficient statistical method for image noise level estimation. In *Proceedings of the IEEE International Conference on Computer Vision*, pages 477–485, 2015.
- Prescott Lecky. Self-consistency; a theory of personality. 1945.
- Kaiming He, Xiangyu Zhang, Shaoqing Ren, and Jian Sun. Deep residual learning for image recognition. In *Proceedings of the IEEE conference on computer vision and pattern recognition*, pages 770–778, 2016.
- Olaf Ronneberger, Philipp Fischer, and Thomas Brox. U-net: Convolutional networks for biomedical image segmentation. In *Medical image computing and computer-assisted intervention–MICCAI 2015: 18th international conference, Munich, Germany, October 5-9, 2015, proceedings, part III 18*, pages 234–241. Springer, 2015.
- Dmitry Ulyanov, Andrea Vedaldi, and Victor Lempitsky. Deep image prior. In *Proceedings of the IEEE conference on computer vision and pattern recognition*, pages 9446–9454, 2018.
- A Vaswani. Attention is all you need. *Advances in Neural Information Processing Systems*, 2017.
- Ziming Liu, Yixuan Wang, Sachin Vaidya, Fabian Ruehle, James Halverson, Marin Soljačić, Thomas Y Hou, and Max Tegmark. Kan: Kolmogorov-arnold networks. *arXiv preprint arXiv:2404.19756*, 2024.